Synsint Research Group

Available online at www.synsint.com

Synthesis and Sintering

ISSN 2564-0186 (Print), **ISSN** 2564-0194 (Online)

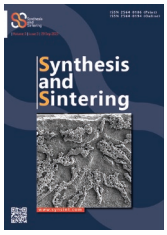

Research article

Corrosion behavior of TiN and TiCN coatings synthesized by PVD on the spark plasma sintered NiTi substrate

Nasim Botshekanan, Hudsa Majidian *, Mohammad Farvizi

Ceramics Department, Materials and Energy Research Center (MERC), Karaj, Iran

A B S T R A C T

TiN and TiCN coatings have garnered widespread attentions in the field of materials science and engineering because of their exceptional characteristics, including high melting point, excellent thermal conductivity, remarkable chemical stability, superior corrosion and wear resistance, and notable biocompatibility. These properties make them highly suitable for coating various alloys, and as a result, they have been successfully applied in numerous applications. The aim of this research study is to delve into the corrosion behavior of spark plasma sintered NiTi substrates that were coated with TiN and TiCN employing physical vapor deposition (cathodic arc technology). In order to comprehensively analyze the corrosion response, potentiodynamic polarization and electrochemical impedance spectroscopy techniques were employed. To gain deeper insights into the impact of the coating, a meticulous comparison was conducted between the corrosion resistance of the uncoated specimen and that of the coated ones. The results showcased a significant enhancement in corrosion resistance for both coated samples when compared to the uncoated NiTi substrate. However, it was found that the TiN-coated specimen showed even higher corrosion resistance than the TiCN-coated counterpart. These findings highlight the superiority of TiN coatings in terms of corrosion resistance when applied on the NiTi substrate.

KEYWORDS

Corrosion resistance
TiN/TiCN coatings
Spark plasma sintering
Physical vapor deposition
NiTi alloys

OPEN ACCESS

1. Introduction

Hard coatings with thicknesses of several micrometers are widely used to boost the performance of cutting, forming, or casting tools and machines. Improving the surface properties of these coatings has always been of great importance in the industry and various research works have been conducted in this regard; However, due to the harsh working conditions, the need to fabricate more resistant coatings against wear and corrosion is felt [1–4]. The applications of hard coatings applied by physical vapor deposition are increasing day by day because of their wear resistance, high hardness, and remarkable corrosion resistance [5–7].

Among the hard coatings, titanium nitride (TiN) is widely used in engineering applications to keep the parts against chemical and mechanical damage [8–11]. TiN coatings have features such as high melting point, chemical stability, corrosion resistance, wear resistance, and biocompatibility. In addition, its beautiful color is appropriate for decorative purposes [12, 13]. To boost the corrosion resistance of TiN coatings, the use of Ti metal intermediate layers is very effective. These intermediate layers enhance corrosion and wear resistance [14].

In recent years, multilayer coatings have been used to achieve coatings with excellent surface properties. These multi-layered coatings offer excellent mechanical, corrosion, and surface properties compared to single-layer coatings, and such an improvement in the properties is attributed to the multilayer structure of these coatings [15–17]. One of the advantages of the multi-layer coating compared to single-layer ones is that in single-layer coatings, the increase in hardness increases the fragility and decreases the efficiency of the coating as the cracks are

* Corresponding author. *E-mail address:* h-majidian@merc.ac.ir (H. Majidian)

Received 9 July 2023; Received in revised form 25 September 2023; Accepted 26 September 2023.

https://doi.org/10.53063/synsint.2023.33166

formed and spread between the coating and the surface of the coating. In multilayer coatings, internal and surface cracks can be controlled, or their direction can be changed [18].

NiTi alloys are well known because they combine inimitable mechanical and physical properties including shape memory effect, high resistance to corrosion and fatigue, super-elasticity, and good strength. In recent decades, this material has been broadly used as a suitable candidate in biomedical usages owing to its aforesaid feathers [19–23]. Up to now, NiTi alloy has been utilized in the cardiovascular, orthopedics, and orthodontics fields as non-vascular and vascular stenting, fixation plates for bone fractures and nails. Hence, NiTi alloy is known as one of the bioinert materials that not only shows weak osteoinductive characteristics when used in living organisms but also corrosion and wear easily occur between them under the influence of physiological environment and human load [24–28]. In addition, the high content of nickel in the alloy is of high concern due to its biocompatibility, since the release of nickel is a potential risk that can cause allergic and toxic reactions [29, 30]. Therefore, to dominate such problems in NiTi alloys, surface treatment methods have been utilized to inhibit Ni ion release and improve their corrosion resistance.

Many works have been done to modify the surface characteristics of NiTi alloy. Surface coating is an effective way to enhance the durability of substrate materials in aggressive environments. Therefore, by choosing suitable coating methods and materials, the life of the substrate material can be increased [31–34]. Various coatings have been applied in different ways on the surface of NiTi, including dense plasma focus, filtered arcing ion plate, physical vapor deposition, and plasma immersion ion implantation and deposition [35–41].

Due to the importance of the subject and the aforementioned cases, this research is done in three stages, in which the NiTi substrates are first manufactured by spark plasma sintering (SPS), then the TiN and TiCN coatings are applied on them by cathodic arc physical vapor deposition (PVD), and finally, the characterizations are carried out. This paper focuses on the corrosion behavior of the mentioned system.

2. Experimental procedure

2.1. Materials and process

To prepare the NiTi substrate, the SPS method was used to sinter the powder, and the process conditions were optimized so that the sintering of the powders led to the fabrication of almost entirely dense samples. For this purpose, spherical Ni and Ti powders with a purity of 99.9% and an average size of 15 μm were used as raw materials. To prepare the powder mixture, a planetary ball mill with a weight ratio of ball to powder of 10:1 was used under an argon gas atmosphere with a rotation speed of 300 rpm for 3 h. The SPS process was performed at the temperature range of 900–1050 °C with a heating rate of 50 °C/min soaking time of 5 min under a pressure of 30 MPa in vacuum. The sintered NiTi pellets had a diameter of 10 mm and a thickness of 3 mm.

The nano-scale PVD coatings were applied with cathodic arc technology, in which an electric arc is used to vaporize particles from the cathodic target to sit on the substrate and form a dense thin layer. In the beginning, the temperature was set to 180 °C to heat the substrate, which was controlled until the end of the layering. The coating time lasted a total of 30 min, the first 15 min of which was to reach the appropriate vacuum in the chamber. Then, the plasma stage started using argon, which was done for 10 min to clean the surface of the substrate and also for better adhesion of the coating on the substrate. Next, deposition was done by creating an intermediate layer between the substrate and the coating to increase adhesion, reduce residual stress, and decrease the thermal expansion coefficient difference between the substrate and the final coating. The initial layer was Ti, which by introducing argon gas into the chamber and applying voltage on the target caused titanium particles to be removed from its surface in the form of vapor so that they were deposited on the substrate for 1 min. After Ti deposition, nitrogen was employed to react with the Ti particles separated from the target to synthesize the final TiN coating in 4 min. In addition, acetylene-nitrogen mixture was used for the synthesis of TiCN as the final coating on one of the samples.

2.2. Characterization

In order to prepare the surface of the specimens for corrosion tests, sandpaper was used for cleaning and then ethanol and distilled water were utilized for washing. Corrosion tests used include electrochemical impedance spectroscopy (EIS), open circuit potential (OCP), and potentiodynamic polarization.

First, the samples were placed in phosphate-buffered saline (PBS) solution and after the potential was stabilized, OCP was measured. Then the EIS test was done based on ASTM G106 in the frequency range of 0.01 to 100000 Hz using a sinusoidal signal with a potential range of -0.7 to +0.7 for four different time intervals (1, 24, 48, and 72 h). ZView (version 1.3) software was employed for data extraction and analysis. The outcomes were displayed as Nyquist, Bode, and Bode-phase diagrams.

To study the corrosion response of the specimens, the potentiodynamic polarization test was performed according to ASTM G5. For this purpose, a potentiostat/galvanostat instrument (EG&G Princeton Applied Research 273A) was used. Before placing the sample in the solution, the area of the sample was determined, and the rest was covered by an insulating material. This action was done in order that when the sample is placed in the solution to perform the corrosion test, only the part in question is exposed to the solution. The samples were the working electrode, and the reference electrode was the saturated calomel. A platinum rod was also used as a counter electrode. Before starting the experiment and establishing the voltage, the samples were placed in PBS solution (1 M) for 1 h to establish the open circuit potential. All tests were performed at a speed of 1 mV/s. The Tafel polarization curves were drawn by the software in the range of -0.8 to +1.5 V. Corrosion current density, corrosion potential, and slopes of anodic and cathodic Tafel lines were measured by PowerSuite software.

Finally, a MIRA3 TESCAN scanning electron microscope was used for microstructural investigations, and an EDS detector was employed to analyze the elemental distribution.

3. Results and discussion

The Tafel polarization diagrams and the data obtained from the potentiodynamic polarization test for NiTi samples, without coating as well as with TiCN and TiN coatings, are presented in Fig. 1 and Table 1, respectively. Based on the obtained results, it may be claimed that the corrosion resistance of NiTi specimens with TiN and TiCN coatings is higher due to having the lowest corrosion current density (0.3 and 0.5 $\mu A/cm^2$) compared to the uncoated sample (7.6 $\mu A/cm^2$).

Table 1. The results of Tafel extrapolation from the potentiodynamic polarization curves.

Sample	Open circuit potential (V)	Corrosion potential (V)	Anodic slope (mV)	Cathodic slope (mV)	Corrosion current density (μA/cm^2)
Uncoated NiTi	-0.560	-0.555	1.120	0.042	7.6
TiN-coated NiTi	-0.574	-0.575	1.157	0.053	0.3
TiCN-coated NiTi	-0.585	-0.586	13.395	19.924	0.5

In other words, coated samples have a more passive nature than the uncoated sample. Also, according to this figure, in the potentiodynamic polarization curve of the uncoated NiTi sample, no passive behavior is observed in the anodic branch. The absence of passive behavior may be due to the uniform corrosion of the NiTi alloy in the anodic branch. Oxygen and hydrogen reduction reactions also occur in the cathode branch. In the samples coated with TiN and TiCN, the passivity of the coating causes high corrosion resistance in NiTi alloy. According to the literature, the reason for this issue is more surface oxidation in the PBS solution for TiN and TiCN coating than for uncoated NiTi [42, 43].

In the following, the impedance test taken at four different times will be examined and compared for TiN- and TiCN-coated and uncoated NiTi samples. It should be noted that the criterion for comparing corrosion resistance in impedance curves is the diameter of the Nyquist diagram and also the amount of impedance at the lowest frequency in the Bode diagram. Thus, the increase in the diameter of the Nyquist diagram indicates the enhancement in the corrosion resistance of the samples. Also, the amount of impedance at the lowest frequency indicates the sum of the resistances in the equivalent circuit of the samples. Therefore, the higher the impedance at the lowest frequency in the Bode diagram, the higher the resistance to corrosion. The time-constant behavior in these samples can be recognized from the phase angle diagram in terms of frequency. Thus, if a peak appears in these diagrams, it indicates that the equivalent circuit of the samples has a time constant (capacitive behavior). This constant is related to the double-layer capacitance behavior.

As shown in Fig. 2, the electrochemical reactions of the uncoated NiTi sample have a time constant at different immersion times. Therefore, no continuous oxidized layer was synthesized as a protective layer during the investigated immersion periods. Moreover, the radius of the semicircle in the Nyquist diagram of this specimen has lessened after 24 h, which indicates a drop in corrosion resistance during this period. Such an observation may be attributed to the loss of the non-uniform oxide layer on the sample surface, which can occur in corrosive environments, especially in the presence of chlorine. The impedance of the sample increases after 48 h of immersion and decreases again after 72 h, which verifies the re-formation and destruction of the non-uniform oxide layer on the sample surface [42, 43].

According to Fig. 3, comparing the electrochemical impedance diagrams of NiTi samples coated with TiN and TiCN, it can be seen that the sample coated with TiN has generally more corrosion resistance than the one coated with TiCN.

The impedance spectrum at different immersion times of the TiN-coated NiTi sample shows that after 24 h of immersion in PBS solution, the corrosion resistance of this sample has increased. This behavior is due to the synthesis of an integrated passive layer on the surface of the coating. After 48 h of immersion, it is observed that the corrosion resistance of the specimen has decreased, which could be due

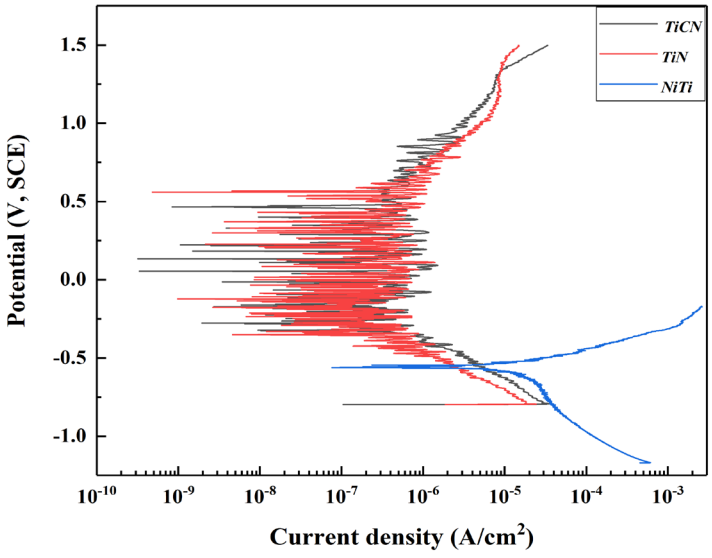

Fig. 1. Potentiodynamic polarization curves after 1-h immersion in PBS solution for uncoated, TiCN-coated, and TiN-coated NiTi samples.

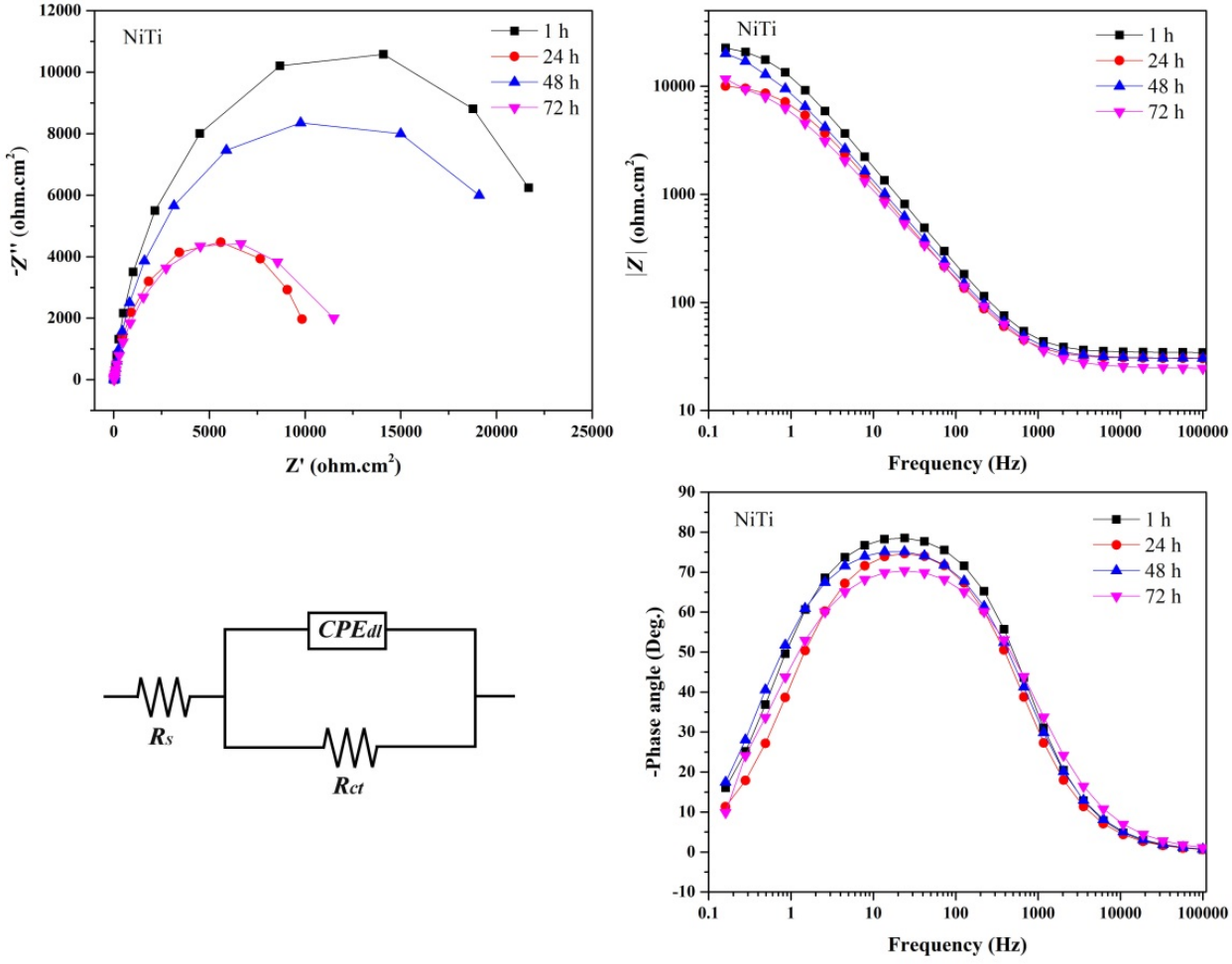

Fig. 2. Electrochemical impedance test for uncoated NiTi sample at different immersion times.

to the destruction of the passive oxide layer. After 72 h, an increase in corrosion resistance is observed that is due to the re-formation of the protective oxide layer on the coating surface.

In the NiTi sample coated with TiCN, it can be observed that the corrosion resistance has decreased after 24 h of immersion in PBS solution. After 48 h of immersion, a further drop in corrosion resistance can be seen in this sample. This amount increased again after 72 h of immersion. The reason for the decrease in corrosion resistance of this sample at immersion times of 24 h and 48 h can be due to the partial destruction of the coating due to the presence of porosity and defects, which is confirmed by microstructural studies. The increase in corrosion resistance after 72 h can be due to the synthesis of a protective oxide layer on the coating or substrate surface.

Quantitative results extracted from the impedance diagrams of all specimens are summarized in Table 2. In this table, R_s represents the resistance of the solution, R_{ct} shows the charge transfer resistance, and CPE_{dl} is the constant phase element (capacitor) attributed to the double layer. In fact, CPE_{dl} is a non-ideal capacitor that is caused by surface roughness in the sample and results in some deviation from the capacitive behavior. Therefore, a constant named "n" is defined, which expresses the degree of deviation from the ideal capacitor, and the closer this value is to 1, the smaller the deviation in the constant phase element.

The microscopic images taken with SEM and EDS analyses performed on uncoated NiTi surfaces as well as coated samples are provided in Figs. 4–6.

As can be observed in Fig. 4, in the uncoated NiTi sample, holes have been created on the surface, and this pitting along with surface oxidation has caused more corrosion in this sample than the coated ones. Identification of oxygen along with nickel and titanium by elemental analysis indicates surface oxidation and corrosion. In Fig. 4, localized corrosion can be seen on the surface of the sample because of the absence of a uniform protective oxide layer. Hence, the localized corrosion can be proposed as the dominant corrosive mechanism in this specimen.

According to Fig. 5, in the sample coated with TiN, the amount of holes in the coating is less and the coating itself has suffered less damage. This means that the sample is mostly passive. Also, the EDS analysis on the surface of the coating discloses the absence of oxygen on the surface of this coating. Therefore, based on the polarization and impedance diagrams, it can be stated that the passive layer formed in this sample is created at the interface of the substrate with the coating.

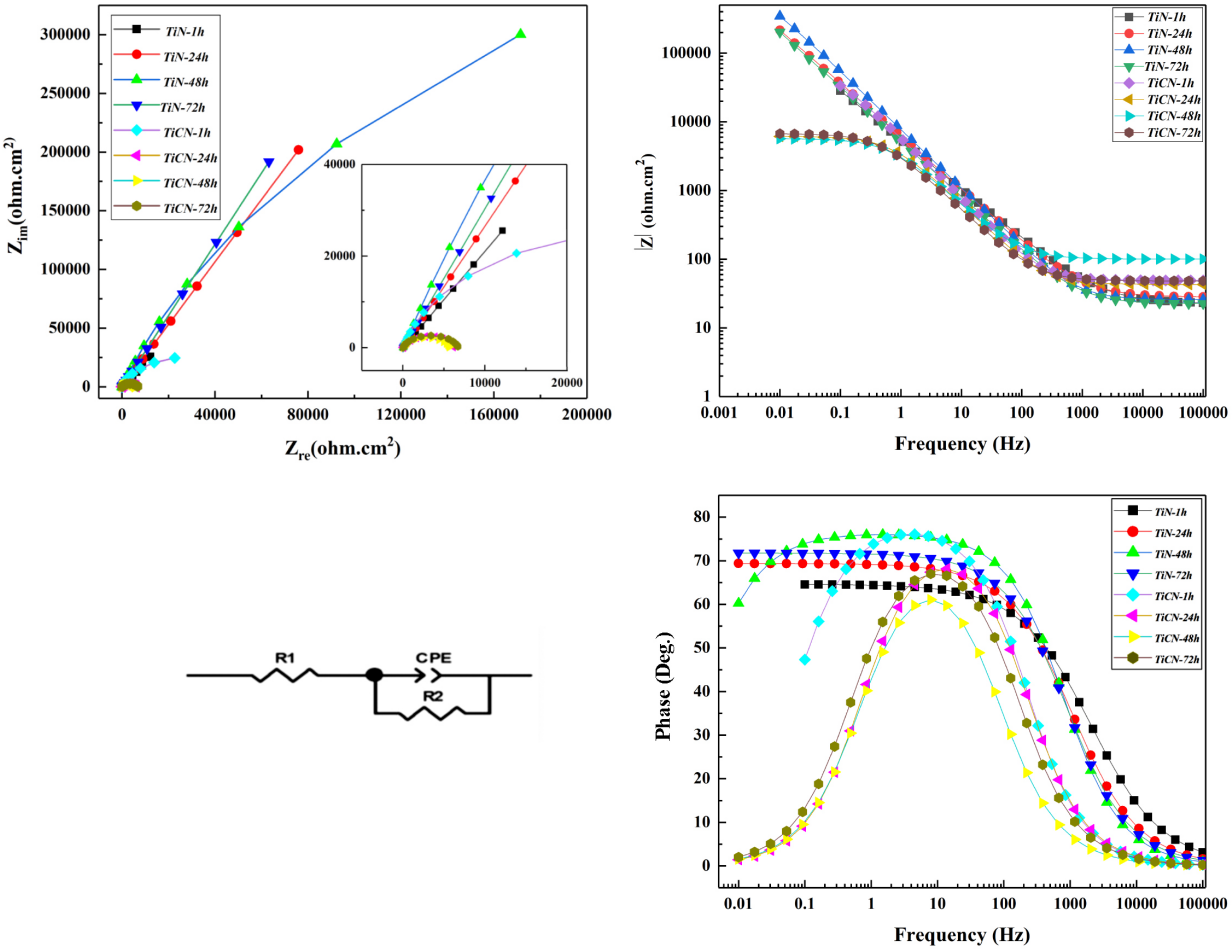

Fig. 3. Electrochemical impedance tests for uncoated NiTi sample sample with TiN and TiCN coatings at immersion times of 1, 24, 48, and 72 h.

The reason for this issue can be attributed to the penetration of oxygen ions in the defects of the coating and the reaching of the ions to the substrate.

It can be deduced from Fig. 6 that pitting has occurred in the NiTi sample coated with TiCN, which is a highly localized type of corrosion that may cause holes in the bulk sample. Pitting can be considered something between uniform corrosion and complete resistance against corrosion, which occurs as a result of a unique autocatalytic anodic reaction. In fact, the corrosion reactions inside the cavity create conditions that stimulate the continuation of the corrosive processes. Here, the TiCN coating is subjected to pitting by PBS solution. Rapid dissolution of the coating is located inside the cavity while oxygen regeneration is done on the adjacent surface. Hydrogen and chlorine ions accelerate the dissolution, and the acceleration of the reaction increases over time. Because the ability to dissolve oxygen in concentrated solutions is almost zero, no oxygen regeneration takes place inside the cavity. The cathodic reaction of oxygen regeneration on the adjacent outer surface protects those surfaces against corrosion.

Table 2. Numerical parameters of impedance test for NiTi, TiN, and TiCN samples after immersion in PBS solution at four different times.

Sample	R_s ($\Omega.cm^2$)	R_{ct} ($k\Omega.cm^2$)	CPE_{dl} ($\Omega^{-1}.cm^{-2}.s^n$)	n
TiN- 1 h	23.6	1.3×10^{13}	4.9×10^{-5}	0.7
TiN- 24 h	28.17	1.8×10^{13}	3.9×10^{-5}	0.7
TiN- 48 h	25.86	1.6×10^{6}	2.7×10^{-5}	0.8
TiN- 72 h	23.42	1.7×10^{13}	4.4×10^{-5}	0.7
TiCN- 1 h	49.04	62149	3.3×10^{-5}	0.8
TiCN- 24 h	42.83	6134	4.4×10^{-5}	0.8
TiCN- 48 h	100.40	5624	5.1×10^{-5}	0.8
TiCN- 72 h	48.24	6720	5.6×10^{-5}	0.8
NiTi- 1 h	34.39	24.33	1.22×10^{-5}	0.91
NiTi- 24 h	30.27	10.55	1.97×10^{-5}	0.89
NiTi- 48 h	30.47	20.05	1.90×10^{-5}	0.88
NiTi- 72 h	24.46	11.60	2.8×10^{-5}	0.83

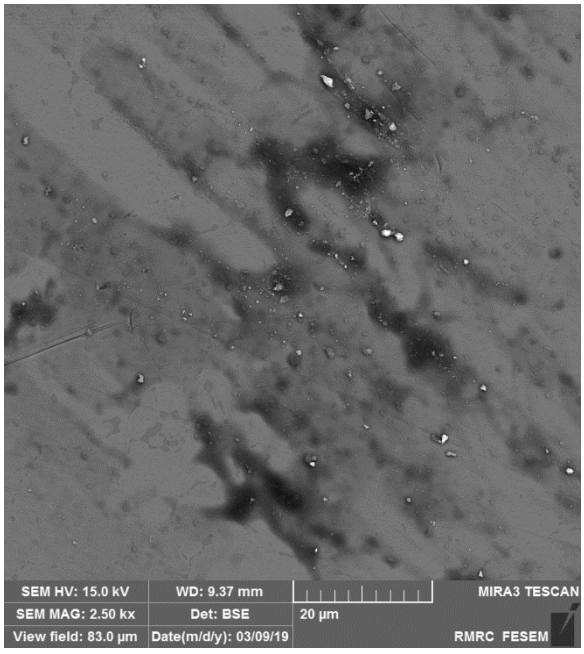

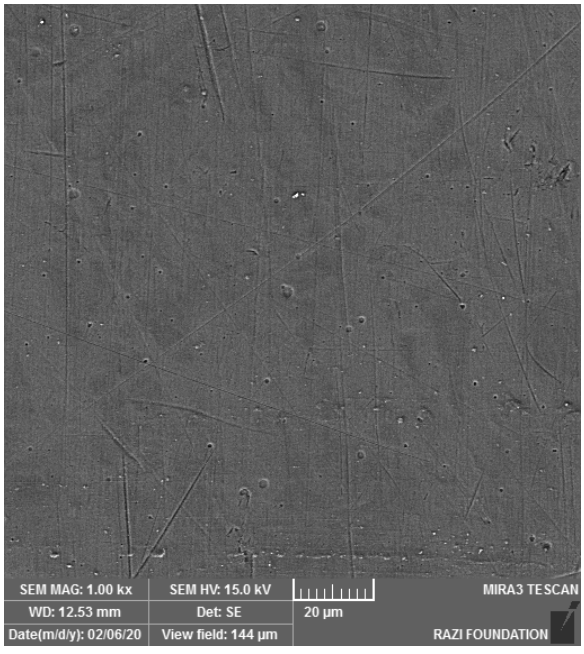

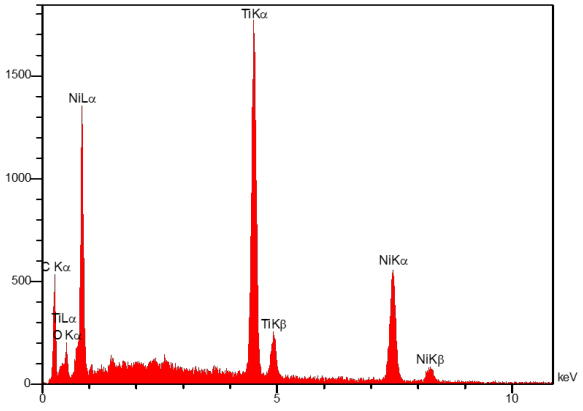

Fig. 4. Surface morphology and EDS result of NiTi after polarization test in PBS solution.

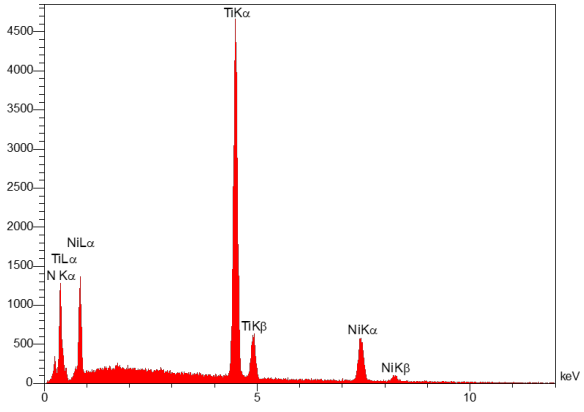

Fig. 5. SEM/EDS results of the surface of TiN-coated NiTi after polarization test in PBS solution.

In other words, the holes provide cathodic protection for the rest of the metal or coating surface.

The mechanism of this type of corrosion can be such that first the oxygen in the environment is regenerated and causes metal oxidation according to Eq. 1, where M represents the metal element. Since the area under the coating is not directly in contact with the solution, this reaction continues until the oxygen in that area is exhausted (Eq. 2). As stated in Eq. 3, when oxygen runs out between the coating and the substrate, chlorine ions react with metal ions and form metal chloride. According to Eq. 4, metal chloride is hydrolyzed in water and turns into metal hydroxide (MOH). In addition to the formation of metal hydroxide, HCl is produced, which causes a local decrease in pH and acidification of the environment (Eq. 4), hence, the corrosion is intensified.

$$M \rightarrow M^{+} + e^{-} \quad (1)$$

$$O_2 + 2H_2O + 4e^{-} \rightarrow 4OH^{-} \quad (2)$$

$$M^{+} + Cl^{-} \rightarrow MCl \quad (3)$$

$$MCl + H_2O \rightarrow MOH + HCl \quad (4)$$

It is obvious that if the coating is free of point defects, porosities, and places of electrolyte penetration to the substrate, and also if the coating adhesion to the substrate is not weak, this type of corrosion will not happen. The lower corrosion resistance of this sample compared to the sample coated with TiN can be seen from the comparison of FESEM images. The EDS analysis of the surface of the TiCN-coated sample also confirms the presence of oxygen, which indicates local corrosion in this coating. It should be noted that oxygen was not detected in the sample coated with TiN.

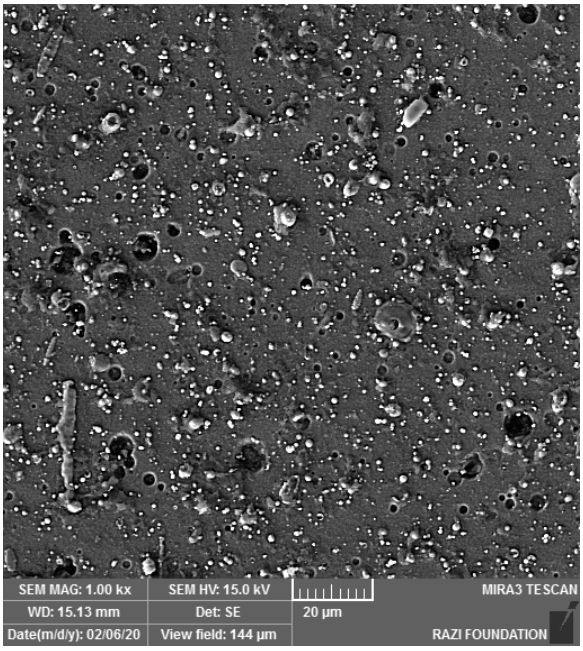

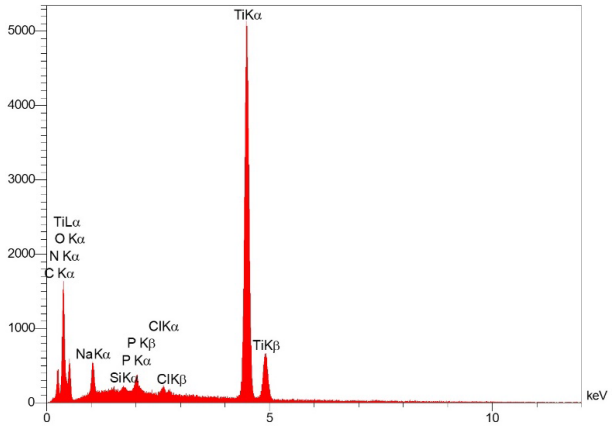

Fig. 6. SEM/EDS results of the surface of TiCN-coated NiTi after polarization test in PBS solution.

4. Conclusions

This research aimed to evaluate the corrosion resistance of spark plasma sintered NiTi substrates coated with TiN and TiCN using cathodic arc technology. The corrosion behavior of the coated specimens was evaluated with electrochemical impedance spectroscopy and potentiodynamic polarization methodologies. It was observed that the corrosion resistance of both coated samples was superior to that of the uncoated NiTi substrate. However, the TiN-coated specimen exhibited even higher corrosion resistance compared to the TiCN-coated one. These findings suggest that the TiN coating, created by physical vapor deposition, outperforms the TiCN coating in terms of corrosion resistance when applied to spark plasma sintered NiTi substrates. Therefore, TiN coatings can be considered as a more suitable and effective choice for enhancing the corrosion resistance of NiTi alloys.

CRediT authorship contribution statement

Nasim Botshekanan: Investigation, Methodology, Writing – original draft.

Hudsa Majidian: Conceptualization, Project administration, Writing – review & editing.

Mohammad Farvizi: Resources, Supervision, Writing – review & editing.

Data availability

The data underlying this article will be shared on reasonable request to the corresponding author.

Declaration of competing interest

The authors declare no competing interests.

Funding and acknowledgment

The paper is derived from the first author's master's thesis. This work was supported by the Materials and Energy Research Center under grant number 371397059.

References

[1] N. Schalk, M. Tkadletz, C. Mitterer, Hard coatings for cutting applications: Physical vs. chemical vapor deposition and future challenges for the coatings community, Surf. Coat. Technol. 429 (2022) 127949. https://doi.org/10.1016/j.surfcoat.2021.127949.

[2] W. Giurlani, E. Berretti, M. Innocenti, A. Lavacchi, Measuring the thickness of metal coatings: A review of the methods, Coatings. 10 (2020) 1211. https://doi.org/10.3390/coatings10121211.

[3] S. Wang, C. Ma, F.C. Walsh, Alternative tribological coatings to electrodeposited hard chromium: a critical review, Trans. IMF. 98 (2020) 173–185. https://doi.org/10.1080/00202967.2020.1776962.

[4] M. Akhlaghi, E. Salahi, S.A. Tayebifard, G. Schmidt, Role of SPS temperature and holding time on the properties of Ti3AlC2-doped TiAl composites, Synth. Sinter. 2 (2022) 138–145. https://doi.org/10.53063/synsint.2022.2383.

[5] J.N. Oliver, Y. Su, X. Lu, P.-H. Kuo, J. Du, D. Zhu, Bioactive glass coatings on metallic implants for biomedical applications, Bioact. Mater. 4 (2019) 261–270. https://doi.org/10.1016/j.bioactmat.2019.09.002.

[6] Y. Deng, W. Chen, B. Li, C. Wang, T. Kuang, Y. Li, Physical vapor deposition technology for coated cutting tools: A review, Ceram. Int. 46 (2020) 18373–18390. https://doi.org/10.1016/j.ceramint.2020.04.168.

[7] F.C. Walsh, S. Wang, N. Zhou, The electrodeposition of composite coatings: Diversity, applications and challenges, Curr. Opin. Electrochem. 20 (2020) 8–19. https://doi.org/10.1016/j.coelec.2020.01.011.

[8] A. Kilicaslan, O. Zabeida, E. Bousser, T. Schmitt, J.E. Klemberg-Sapieha, L. Martinu, Hard titanium nitride coating deposition inside narrow tubes using pulsed DC PECVD processes, Surf. Coat. Technol. 377 (2019) 124894. https://doi.org/10.1016/j.surfcoat.2019.124894.

[9] M. Łępicka, M. Grądzka-Dahlke, D. Pieniak, K. Pasierbiewicz, K. Kryńska, A. Niewczas, Tribological performance of titanium nitride coatings: A comparative study on TiN-coated stainless steel and titanium alloy, Wear. 422–423 (2019) 68–80. https://doi.org/10.1016/j.wear.2019.01.029.

[10] A. Ghailane, M. Makha, H. Larhlimi, J. Alami, Design of hard coatings deposited by HiPIMS and dcMS, Mater. Lett. 280 (2020) 128540. https://doi.org/10.1016/j.matlet.2020.128540.

[11] A. Shima, M. Kazemi, Influence of TiN addition on densification behavior and mechanical properties of ZrB2 ceramics, Synth. Sinter. 3 (2023) 46–53. https://doi.org/10.53063/synsint.2023.31133.
[12] A. Kumar, R.S. Mulik, Improving tribological behavior of titanium nitride (TiN) hard coatings via zirconium (Zr) or vanadium (V) doping, Tribol. Int. 189 (2023) 108997. https://doi.org/10.1016/j.triboint.2023.108997.
[13] I. Çaha, A.C. Alves, L.J. Affonço, P.N. Lisboa-Filho, J.H.D. da Silva, et al., Corrosion and tribocorrosion behaviour of titanium nitride thin films grown on titanium under different deposition times, Surf. Coat. Technol. 374 (2019) 878–888. https://doi.org/10.1016/j.surfcoat.2019.06.073.
[14] J. Vega, H. Scheerer, G. Andersohn, M. Oechsner, Experimental studies of the effect of Ti interlayers on the corrosion resistance of TiN PVD coatings by using electrochemical methods, Corros. Sci. 133 (2018) 240–250. https://doi.org/10.1016/j.corsci.2018.01.010.
[15] P.G. Grützmacher, S. Suarez, A. Tolosa, C. Gachot, G. Song, et al., Superior wear-resistance of Ti3C2Tx multilayer coatings, ACS Nano. 15 (2021) 8216–8224. https://doi.org/10.1021/acsnano.1c01555.
[16] J.W. Du, L. Chen, J. Chen, Y. Du, Mechanical properties, thermal stability and oxidation resistance of TiN/CrN multilayer coatings, Vacuum. 179 (2020) 109468. https://doi.org/10.1016/j.vacuum.2020.109468.
[17] M.S. Safavi, M.A. Surmeneva, R.A. Surmenev, J. Khalil-Allafi, RF-magnetron sputter deposited hydroxyapatite-based composite and multilayer coatings: A systematic review from mechanical, corrosion, and biological points of view, Ceram. Int. 47 (2021) 3031–3053. https://doi.org/10.1016/j.ceramint.2020.09.274.
[18] A. Gilewicz, B. Warcholinski, Tribological properties of CrCN/CrN multilayer coatings, Tribol. Int. 80 (2014) 34–40. https://doi.org/10.1016/j.triboint.2014.06.012.
[19] S.K. Patel, B. Behera, B. Swain, R. Roshan, D. Sahoo, A. Behera, A review on NiTi alloys for biomedical applications and their biocompatibility, Mater. Today Proc. 33 (2020) 5548–5551. https://doi.org/10.1016/j.matpr.2020.03.538.
[20] R. Hang, F. Zhao, X. Yao, B. Tang, P.K. Chu, Self-assembled anodization of NiTi alloys for biomedical applications, Appl. Surf. Sci. 517 (2020) 146118. https://doi.org/10.1016/j.apsusc.2020.146118.
[21] K. Safaei, H. Abedi, M. Nematollahi, F. Kordizadeh, H. Dabbaghi, et al., Additive manufacturing of NiTi shape memory alloy for biomedical applications: review of the LPBF process ecosystem, JOM. 73 (2021) 3771–3786. https://doi.org/10.1007/s11837-021-04937-y.
[22] S. Kumar Patel, B. Swain, R. Roshan, N.K. Sahu, A. Behera, A brief review of shape memory effects and fabrication processes of NiTi shape memory alloys, Mater. Today Proc. 33 (2020) 5552–5556. https://doi.org/10.1016/j.matpr.2020.03.539.
[23] H. Aghajani, A. Taghizadeh Tabrizi, S. Arabpour Javadi, M.E. Taghizadeh Tabrizi, A. Homayouni, S. Behrangi, Thermodynamically study of phase formation of Ni-Ti-Si nanocomposites produced by self-propagating high-temperature synthesis method, Synth. Sinter. 1 (2021) 189–196. https://doi.org/10.53063/synsint.2021.1443.
[24] A. Kapanen, J. Ilvesaro, A. Danilov, J. Ryhänen, P. Lehenkari, J. Tuukkanen, Behaviour of Nitinol in osteoblast-like ROS-17 cell cultures, Biomaterials. 23 (2002) 645–650. https://doi.org/10.1016/S0142-9612(01)00143-0.
[25] J.D. Weaver, L. Ramirez, S. Sivan, M. Di Prima, Characterizing fretting damage in different test media for cardiovascular device durability testing, J. Mech. Behav. Biomed. Mater. 82 (2018) 338–344. https://doi.org/10.1016/j.jmbbm.2018.04.004.
[26] Q. Liu, M. Liu, Y. Tian, J. Cheng, J. Lang, et al., Evaluation of resistance to radial cyclic loads of poly(L-lactic acid) braided stents with different braiding angles, Int. J. Biol. Macromol. 218 (2022) 94–101. https://doi.org/10.1016/j.ijbiomac.2022.07.107.
[27] R.M.F. Wagner, R. Maiti, M.J. Carré, C.M. Perrault, P.C. Evans, R. Lewis, Bio-tribology of vascular devices: A review of tissue/device friction research, Biotribology. 25 (2021) 100169. https://doi.org/10.1016/j.biotri.2021.100169.
[28] E.R. Clark, K.E. Porter, M.G. Bryant, Fretting-corrosion of cardiovascular stent materials: The role of electrochemical polarisation on debris generation mechanisms, Biotribology. 18 (2019) 100093. https://doi.org/10.1016/j.biotri.2019.100093.
[29] X. Lü, X. Bao, Y. Huang, Y. Qu, H. Lu, Z. Lu, Mechanisms of cytotoxicity of nickel ions based on gene expression profiles, Biomaterials. 30 (2009) 141–148. https://doi.org/10.1016/j.biomaterials.2008.09.011.
[30] B. Subramanian, C.V. Muraleedharan, R. Ananthakumar, M. Jayachandran, A comparative study of titanium nitride (TiN), titanium oxy nitride (TiON) and titanium aluminum nitride (TiAlN), as surface coatings for bio implants, Surf. Coat. Technol. 205 (2011) 5014–5020. https://doi.org/10.1016/j.surfcoat.2011.05.004.
[31] Y. Guo, Z. Xu, Q. Wang, S. Zu, M. Liu, et al., Corrosion resistance and biocompatibility of graphene oxide coating on the surface of the additively manufactured NiTi alloy, Prog. Org. Coat. 164 (2022) 106722. https://doi.org/10.1016/j.porgcoat.2022.106722.
[32] M.S. Safavi, A. Bordbar-Khiabani, F.C. Walsh, M. Mozafari, J. Khalil-Allafi, Surface modified NiTi smart biomaterials: Surface engineering and biological compatibility, Curr. Opin. Biomed. Eng. 25 (2023) 100429. https://doi.org/10.1016/j.cobme.2022.100429.
[33] H. Wang, J. Jürgensen, P. Decker, Z. Hu, K. Yan, et al., Corrosion behavior of NiTi alloy subjected to femtosecond laser shock peening without protective coating in air environment, Appl. Surf. Sci. 501 (2020) 144338. https://doi.org/10.1016/j.apsusc.2019.144338.
[34] S. Samal, O. Kosjakova, Surface feature of PMMA films on NiTi alloy substrate by the spin coating method, Ceram. Int. 49 (2023) 24370–24378. https://doi.org/10.1016/j.ceramint.2022.10.152.
[35] L.S. Anthony, V. Perumal, N.M. Mohamed, S.R. Balakrishnan, S.C.B. Gopinath, Characterization of synthesized nanoparticles for medical devices: current techniques and recent advances, Nanoparticles in Analytical and Medical Devices, Elsevier. (2021) 223–245. https://doi.org/10.1016/B978-0-12-821163-2.00012-1.
[36] S. Mohammed, M. Kök, I.N. Qader, M. Coşkun, A review study on biocompatible improvements of NiTi-based shape memory alloys, Int. J. Innov. Eng. Appl. 5 (2021) 125–130. https://doi.org/10.46460/ijiea.957722.
[37] P.K. Chu, Progress in direct-current plasma immersion ion implantation and recent applications of plasma immersion ion implantation and deposition, Surf. Coat. Technol. 229 (2013) 2–11. https://doi.org/10.1016/j.surfcoat.2012.03.073.
[38] T. Lu, Y. Qiao, X. Liu, Surface modification of biomaterials using plasma immersion ion implantation and deposition, Interface Focus. 2 (2012) 325–336. https://doi.org/10.1098/rsfs.2012.0003.
[39] J. Pelletier, A. Anders, Plasma-based ion implantation and deposition: a review of physics, technology, and applications, IEEE Trans. Plasma Sci. 33 (2005) 1944–1959. https://doi.org/10.1109/TPS.2005.860079.
[40] T. Tripi, A. Bonaccorso, G. Condorelli, Fabrication of hard coatings on NiTi instruments, J. Endod. 29 (2003) 132–134. https://doi.org/10.1097/00004770-200302000-00011.
[41] L. Geyao, D. Yang, C. Wanglin, W. Chengyong, Development and application of physical vapor deposited coatings for medical devices: A review, Procedia CIRP. 89 (2020) 250–262. https://doi.org/10.1016/j.procir.2020.05.149.
[42] B.G. Pound, The electrochemical behavior of nitinol in simulated physiological solutions, J. Biomed. Mater. Res. 85A (2008) 1103–1113. https://doi.org/10.1002/jbm.a.31616.
[43] A.W. Hansen, L.T. Führ, L.M. Antonini, D.J. Villarinho, C.E.B. Marino, C. de F. Malfatti, The electrochemical behavior of the NiTi alloy in different simulated body fluids, Mater. Res. 18 (2015) 184–190. https://doi.org/10.1590/1516-1439.305614.